Published in IET Signal Processing
Received on 14th July 2010
Revised on 25th April 2011
doi: 10.1049/iet-spr.2010.0196

ISSN 1751-9675

Joint complex diversity coding and channel coding over space, time and frequency

J. Wu[1,2] *P. Xiao*[3] *M. Sellathurai*[4] *S. Blostein*[1] *T. Ratnarajah*[4]

[1]*Department of Electrical and Computer Engineering, Queen's University, Kingston, Ontario K7L 3N6, Canada*
[2]*Bell Laboratories, Alcatel-Lucent, Shanghai 201206, Peoples Republic of China*
[3]*Centre for Communication Systems Research, University of Surrey, Guildford, Surrey GU2 7XH, UK*
[4]*The Institute of Electronics, Communications and Information Technology, Queen's University Belfast, BT3 9DT, UK*
E-mail: wujs@ieee.org

Abstract: This study provides a general diversity analysis for joint complex diversity coding (CDC) and channel coding-based space-time-frequency codeing is provided. The mapping designs from channel coding to CDC are crucial for efficient exploitation of the diversity potential. This study provides and proves a sufficient condition of full diversity construction with joint three-dimensional CDC and channel coding, bit-interleaved coded complex diversity coding and symbol-interleaved coded complex diversity coding. Both non-iterative and iterative detections of joint channel code and CDC transmission are investigated. The proposed minimum mean-square error-based iterative soft decoding achieves the performance of the soft sphere decoding with reduced complexity.

1 Introduction

A challenging problem in wideband multiple-input multiple-output (MIMO) system design is to develop new high-rate coding schemes to efficiently exploit all the diversity available across space, time and frequency domains. To this end, the design of space-time-frequency coding (STFC) has been recently investigated in [1, 2]. We introduce a general terminology, complex diversity coding (CDC), which summarises existing diversity coding approaches using complex conversion. STFCs may be categorised into different integrations of CDC and channel coding, such as error control coding (ECC). Note that CDC is also called signal space diversity [3] in single-input single-output communications and linear dispersion codes (LDC) in two-dimensional (2D) space time MIMO channels.

Unlike the previous analysis for pure 3D CDC systems presented in [2, 4], this paper provides a general diversity analysis for systems with joint 3D CDC and channel coding. Our diversity analysis also differs from the joint 1D or 2D CDC and channel-coding-related performance analysis (e.g. those conducted in [5, 6]), since we provide a clear construction of full diversity joint 3D CDC and channel coding without assumption of infinite length of the channel code, and the physical dimensions used in our diversity analysis are different from those in [5, 6].

Unlike the computationally prohibitive maximum likelihood (ML) or sphere decoding (SD)-based turbo decoding for joint ECC and 2D CDC in [7], in this paper, a low complexity iterative minimum mean square error (MMSE) inner decoding for high rate 3D CDC-based STFC and Log-MAP outer decoding for ECC is proposed, and is shown to have comparable performance to the non-iterative STFC near-ML sphere decoding.

Notations: $(\cdot)^{\mathcal{T}}$ – the matrix transpose, $(\cdot)^{\mathcal{H}}$ – the matrix transpose conjugate, $E[\cdot]$ – the expectation operation, j – the square root of -1, $\boldsymbol{I}_K$ – the identity matrix of size $K \times K$, $\boldsymbol{0}_{M\times N}$ – the zero matrix of size $M \times N$, $\boldsymbol{A} \otimes \boldsymbol{B}$ – the Kronecker (tensor) product of matrices $\boldsymbol{A}$ and $\boldsymbol{B}$, $[\boldsymbol{A}]_{a,b}$ – the (a, b) entry of matrix $\boldsymbol{A}$, and $(\cdot)$ transforms the argument from a vector to a diagonal matrix, and $\text{vec}(\boldsymbol{X}) - [[[\boldsymbol{X}]_{:,1}]^{\mathcal{T}}, \ldots, [[\boldsymbol{X}]_{:,N}]^{\mathcal{T}}]^{\mathcal{T}}$, where matrix $\boldsymbol{X}$ is of size $M \times N$.

2 Proposed system model

2.1 Space-time-frequency block (STFB) and STFC

The baseband-received signal is formed as shown in Fig. 1. We consider a MIMO–OFDM system with N_t transmit antennas, N_r receive antennas, and a block of N_c orthogonal frequency-division multiplexing (OFDM) subcarriers per antenna. Channel coefficients are assumed to be constant within one OFDM block. However, the channel coefficients change from block to block, and they are assumed to be statistically independent among different OFDM blocks. One 3D CDC-based STFC codeword contains D STFB, each of which is of size $N_t \times N_F \times T$, that is, across N_t transmit antennas N_F subcarriers and T OFDM blocks, where $N_C = DN_F$. The data sequence is modulated using complex-valued symbols $\alpha_q + i\beta_q$, chosen from an arbitrary constellation (e.g. r-PSK or r-QAM). One STFB, denoted by $\boldsymbol{S}_{\text{STFB}}$, can be written in matrix form as

$$\boldsymbol{S}_{\text{STFB}} = \sum_{q=1}^{Q} (\alpha_q \boldsymbol{A}_q + j\beta_q \boldsymbol{B}_q) \tag{1}$$

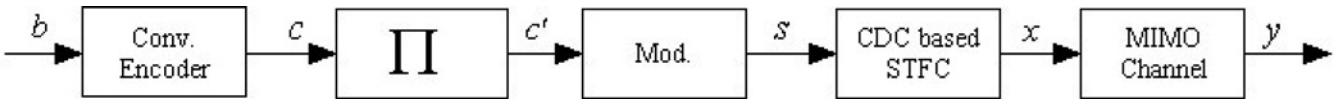

Fig. 1 *Block diagram of the transmitter for the STFC system*

where $\boldsymbol{A}_q \in \mathbb{C}^{N_T \times N_F T}$ and $\boldsymbol{B}_q \in \mathbb{C}^{N_T \times N_F T}$ are dispersion matrices for the real and imaginary parts of source signals. Equation (1) may be considered as a 3D formulation of LDCs [8], and can be reformulated as follows:

1. if $\boldsymbol{A}_q \neq \boldsymbol{B}_q$

$$\text{vec}(\boldsymbol{S}_{\text{STFB}}) = \boldsymbol{G}^{\text{vec}}_{\text{STFB}} \boldsymbol{q} \tag{2}$$

where

$$\boldsymbol{G}^{\text{vec}}_{\text{STFB}} = [\text{vec}(\boldsymbol{A}_1), \ \ldots, \text{vec}(\boldsymbol{A}_Q), \text{jvec}(\boldsymbol{B}_1), \ \ldots, \text{jvec}(\boldsymbol{B}_Q)]$$

$$\boldsymbol{\theta} = [\alpha_1, \ \ldots, \alpha_Q, \beta_1, \ \ldots, \beta_Q]^{\text{T}}$$

2. if $\boldsymbol{A}_q = \boldsymbol{B}_q$,

$$\text{vec}(\boldsymbol{S}_{\text{STFB}}) = \boldsymbol{G}_{\text{STFB}} \boldsymbol{s} \tag{3}$$

where

$$\boldsymbol{G}_{\text{STFB}} = [\text{vec}(\boldsymbol{A}_1), \ \ldots, \text{vec}(\boldsymbol{A}_Q)]$$

$$\boldsymbol{s} = [s_1, \ \ldots, s_Q]^{\text{T}}$$

We define the coding rate of CDC-based STFC as $R^{\text{sym}} = \sum_{i=1}^{D} Q_i/(N_t N_c T)$, where Q_i is the number of source symbols encoded in the ith STFB. In our simulations, we apply rate-one full diversity CDC-based STFCs proposed in [2], and these codes satisfy $\boldsymbol{A}_q = \boldsymbol{B}_q$.

2.2 Frequency domain system model and structure

Consider one joint CDC–ECC STFC block where ECC are across K 3D CDC-based STFC codewords. The baseband frequency domain signal for the ith STFB within the kth STFC can be written as

$$\boldsymbol{y}^{(i,k)} = \sqrt{\frac{\rho}{N_t}} \boldsymbol{H}^{(i,k)}_{\text{STFB}} \boldsymbol{G}_{\text{STFB}} \boldsymbol{s}^{(i,k)} + \boldsymbol{n}^{(i,k)} \tag{4}$$

where $\mathbf{H}^{(i,k)}_{\text{STFB}}$ is the corresponding frequency domain channel matrix of size $N_r N_F T \times N_t N_F T$. Both vectors $\boldsymbol{y}^{(i,k)}$ and $\boldsymbol{n}^{(i,k)}$ are of size $N_r N_F T$, and they are the frequency domain received signal and additive complex Gaussian noise vectors, respectively. The source signal vector $\boldsymbol{s}^{(i,k)}$ is of size $N_t N_F T$. The channel matrix $\boldsymbol{H}^{(i,k)}_{\text{STFB}}$ is formed as

$$\boldsymbol{H}^{(i,k)}_{\text{STFB}} = \text{diag}(\boldsymbol{H}^{(i,1,k)}_{\text{STFB}}, \ \ldots, \boldsymbol{H}^{(i,T,k)}_{\text{STFB}})$$

where $\boldsymbol{H}^{(i,t,k)}_{\text{STFB}} = \text{diag}(\boldsymbol{H}^{(i,t,k)}_{\text{STFB}(p_1)}, \ \ldots, \boldsymbol{H}^{(i,t,k)}_{\text{STFB}(p_{N_F})})$, $\boldsymbol{H}^{(i,t,k)}_{\text{STFB}(p)}$ of size $N_r \times N_t$ is the frequency domain MIMO channel matrix for the pth subcarrier, tth OFDM block, ith STFB, kth CDC-based STFC ($i = 1, \ldots, D$, $t = 1, \ldots, T$, $n_F = 1, \ldots, N_F$, $k = 1, \ldots, K$). $\{p^{(i)}_1, \ \ldots, p^{(i)}_{N_F}\}$ is the subcarrier set chosen for ith CDC-encoded STF block. As shown in Fig. 2, the ECC-coded streams are first interleaved with random interleaver, and mapped into complex source symbols, which are subsequently encoded into CDC-based STFCs (Fig. 3). One set of ECC streams is across K STFCs and N_a STFBs within one STFC.

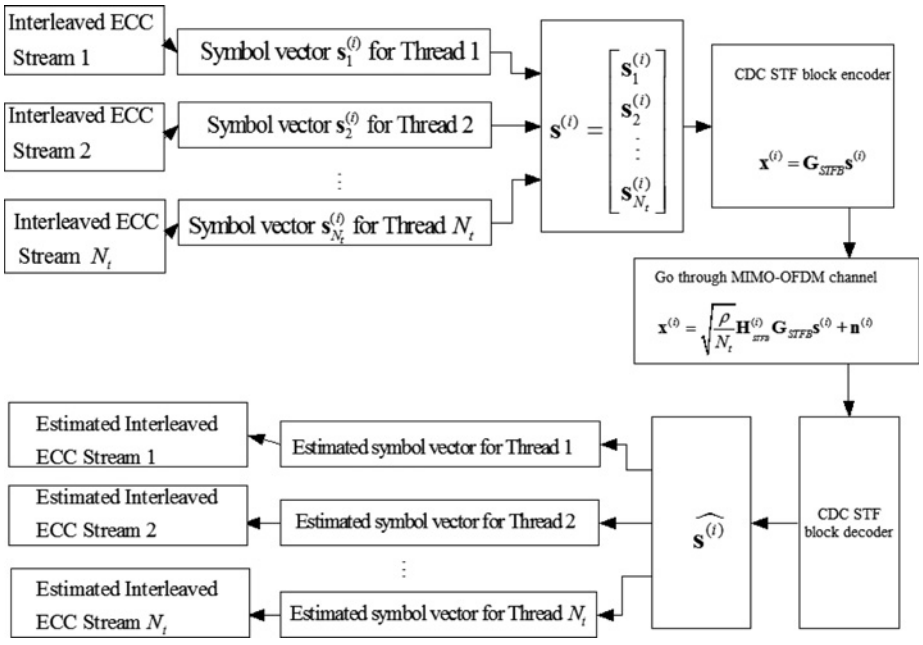

Fig. 2 *Structure of multi-stream joint CDC and ECC STFC*

doi: 10.1049/iet-spr.2010.0196

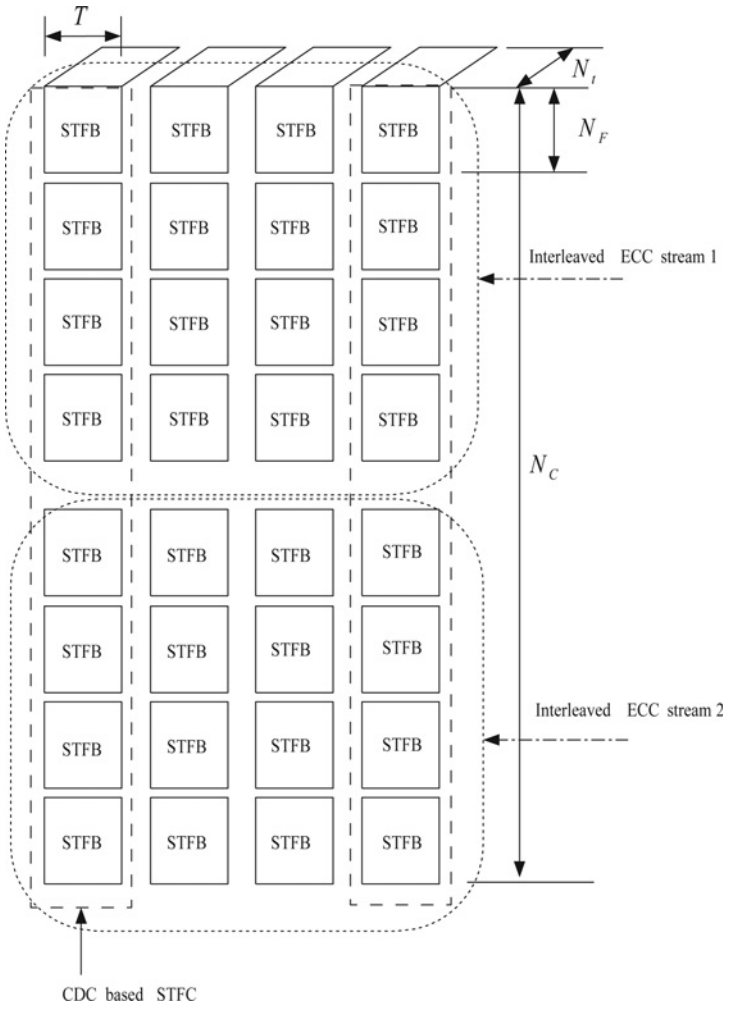

Fig. 3 *Structure of the STFC code*

3 Diversity analysis

We assume that one channel-coding stream is encoded across K STFCs and N_a STFBs per STFC with indices $i = i_1, \ldots, i_{N_a}$. Denote the ith STFB within the kth STFC as $\boldsymbol{C}^{(i,k)}$, which is formed as

$$\boldsymbol{C}^{(i,k)} = [[\boldsymbol{C}^{(1,i,k)}]^{\mathrm{T}} \quad [\boldsymbol{C}^{(2,i,k)}]^{\mathrm{T}} \quad \cdots \quad [\boldsymbol{C}^{(T,i,k)}]^{\mathrm{T}}]^{\mathrm{T}}$$

where $\boldsymbol{C}^{(t,i,k)}$ has entries $[\boldsymbol{C}^{(t,i,k)}]_{a,b} = c^{(t,i,k)}_{b,p_a^{(i)}}$, and $c^{(t,i,k)}_{m,p_{n_{\mathrm{F}}}^{(i)}}$ is the channel symbol of the kth OFDM block, the tth OFDM block, the $p_a^{(i)}$th subcarrier from the mth transmit antenna, and $p_a^{(i)} = p_1^{(i)}, \ldots, p_{N_{\mathrm{F}}}^{(i)}$ is the subcarrier index for the ith STFB. The received signal corresponding to STFB $\boldsymbol{C}^{(i,k)}$ can be reformed as

$$\overline{\boldsymbol{y}}^{(i,k)} = \sqrt{\frac{\rho}{N_{\mathrm{T}}}}\boldsymbol{M}^{(i,k)}\overline{\boldsymbol{H}}^{(i,k)} + \overline{\boldsymbol{v}}^{(i,k)}$$

where $\overline{\boldsymbol{y}}^{(i,k)}$ and $\overline{\boldsymbol{v}}^{(i,k)}$ are the receive signal vector and noise vector, respectively, $\boldsymbol{M}^{(i,k)} = I_{N_{\mathrm{r}}} \otimes [\boldsymbol{M}_1^{(i.k)}, \ldots, \boldsymbol{M}_{N_{\mathrm{t}}}^{(i,k)}]$, and

$$\boldsymbol{M}_m^{(i,k)} = \mathrm{diag}(c^{(1,i,k)}_{m,p_1^{(i)}}, \ldots, c^{(1,i,k)}_{m,p_{N_{\mathrm{F}}}^{(i)}}, \ldots, c^{(T,i,k)}_{m,p_1^{(i)}}, \ldots, c^{(T,i,k)}_{m,p_{N_{\mathrm{F}}}^{(i)}})$$

The equivalent frequency domain channel vector of size $N_{\mathrm{F}}N_{\mathrm{t}}N_{\mathrm{r}}T \times 1$ can be expressed as

$$\overline{\boldsymbol{H}}^{(i,k)} = \left[\begin{array}{c}[\overline{\boldsymbol{H}}^{(i,k)}_{1,1}]^{\mathrm{T}}, \ldots, [\overline{\boldsymbol{H}}^{(i,k)}_{N_{\mathrm{t}},1}]^{\mathrm{T}}, \ldots, [\overline{\boldsymbol{H}}^{(i,k)}_{1,2}]^{\mathrm{T}}, \ldots, [\overline{\boldsymbol{H}}^{(i,k)}_{N_{\mathrm{t}},2}]^{\mathrm{T}}, \\ \ldots, [\overline{\boldsymbol{H}}^{(i,k)}_{1,N_{\mathrm{r}}}]^{\mathrm{T}}, \ldots, [\overline{\boldsymbol{H}}^{(i,k)}_{N_{\mathrm{t}},N_{\mathrm{r}}}]^{\mathrm{T}}\end{array}\right]^{\mathrm{T}}$$

where

$$\overline{\boldsymbol{H}}^{(i,k)}_{m,n} = \left[\begin{array}{c}H^{(1,k)}_{m,n,p_1^{(i)}}, H^{(1,k)}_{m,n,p_2^{(i)}}, \ldots, H^{(1,k)}_{m,n,p_{N_{\mathrm{F}}}^{(i)}}, \ldots, \\ H^{(T,k)}_{m,n,p_1^{(i)}}, H^{(T,k)}_{m,n,p_2^{(i)}}, \ldots, H^{(T,k)}_{m,n,p_{N_{\mathrm{F}}}^{(i)}}\end{array}\right]^{\mathrm{T}}$$

and $H^{(k)}_{m,n,p_{n_{\mathrm{F}}}^{(i)}}$ is the frequency domain channel gain of the kth OFDM block, the $p_{n_{\mathrm{F}}}^{(i)}$ th subcarrier for block between the mth transmit antenna and the nth receive antenna, where $m = 1, \ldots, N_{\mathrm{t}}$ and $n = 1, \ldots, N_{\mathrm{r}}$.

Considering a pair of matrices $\boldsymbol{M}_{(a)}^{(i,k)}$ and $\boldsymbol{M}_{(b)}^{(i,k)}$ which correspond to two different blocks $\boldsymbol{C}_a^{(i,k)}$ and $\boldsymbol{C}_b^{(i,k)}$, the upper bound for the pairwise error probability between

$\boldsymbol{M}_{(a)}^{(i,k)}$ and $\boldsymbol{M}_{(b)}^{(i,k)}$ is [9]

$$\boldsymbol{P}_r\{\boldsymbol{M}_a^{(i,k)} - \boldsymbol{M}_b^{(i,k)}\} \le \binom{2r_{(i,k)} - 1}{r_{(i,k)}} \times \left(\prod_{c=1}^{r_{(i,k)}} \gamma_c^{(i,k)}\right)^{-1} \left(\frac{\rho}{N_t}\right)^{-r_{(i,k)}} \quad (5)$$

where $r_{(i,k)}$ has the rank of

$$\Lambda_{(a,b)}^{(i,k)} = (\boldsymbol{M}_{(a)}^{(i.k)} - \boldsymbol{M}_{(b)}^{(i.k)})\boldsymbol{R}_{\overline{\boldsymbol{H}}^{(i,k)}}(\boldsymbol{M}_{(a)}^{(i.k)} - \boldsymbol{M}_{(b)}^{(i.k)})^{\mathcal{H}}$$

and $\boldsymbol{R}_{\boldsymbol{H}^{(i,k)}} = \mathbb{E}\{\boldsymbol{H}^{(i,k)}[\boldsymbol{H}^{(i,k)}]^{\mathcal{H}}\}$ is correlation matrix of $\boldsymbol{H}^{(i,k)}$, and $\gamma_c^{(i,k)}$, $c = 1, \ldots, r_{(i,k)}$ are the non-zero eigenvalues of $\Lambda_{(a,b)}^{(i,k)}$. Denote $\psi_{(b)}^{(i.k)} = \boldsymbol{M}_{(b)}^{(i.k)} - \boldsymbol{M}_{(b)}^{(i.k)}$, then $\boldsymbol{L}^{(i,k)} = \psi_{(a,b)}^{(i.k)} \boldsymbol{R}_{\overline{\boldsymbol{H}}^{(i,k)}}[\psi_{(a,b)}^{(i.k)}]^{\mathcal{H}}$. Also denote $\psi_{(a,b)} = \text{diag}(\psi_{(a,b)}^{(1)}, \ldots, \psi_{(a,b)}^{(K)})$, $\psi_{(a,b)}^{(k)} = \text{diag}(\psi_{(a,b)}^{(i_1.k)}, \ldots, \psi_{(a,b)}^{(i_{N_a}.k)})$, $\overline{\mathbf{H}} = [[\overline{\mathbf{H}}^{(1)}]^{\mathrm{T}}, \ldots, [\overline{\mathbf{H}}^{(K)}]^{\mathrm{T}}]^{\mathrm{T}}$, $\overline{\mathbf{H}}^{(k)} = [[\overline{\mathbf{H}}^{(i_1,k)}]^{\mathrm{T}}, \ldots, [\overline{\mathbf{H}}^{(i_{N_a},k)}]^{\mathrm{T}}]^{\mathrm{T}}$, $\boldsymbol{R}_{\overline{\boldsymbol{H}}} = \mathbb{E}\{\overline{\boldsymbol{H}}[\overline{\boldsymbol{H}}]^{\mathcal{H}}\}$, $\boldsymbol{M}_{(a)} = \text{diag}(\boldsymbol{M}_{(a)}^{(k)}, \ldots, \boldsymbol{M}_{(a)}^{(k)})$ and $\boldsymbol{M}_{(a)}^{(k)} = \text{diag}\,(\boldsymbol{M}_{(a)}^{(i_1,k)}, \ldots, \boldsymbol{M}_{(a)}^{(i_{N_a},k)})$.

The upper bound of the pairwise error probability between $\boldsymbol{M}_{(a)}$ and $\boldsymbol{M}_{(b)}$ can now be expressed as

$$\boldsymbol{P}_{\mathrm{r}}\{\boldsymbol{M}_{(a)} - \boldsymbol{M}_{(b)}\} \le \binom{2r-1}{r}\left(\prod_{c=1}^{r}\gamma_c\right)^{-1}\left(\frac{\rho}{N_{\mathrm{t}}}\right)^{-r} \quad (6)$$

where r is the rank of $\boldsymbol{\Lambda}_{(a,b)}$, and γ_c, $c = 1, \ldots, r$ are the non-zero eigenvalues of $\boldsymbol{\Lambda}_{(a,b)}$. Note that the upper limit diversity order of this system is

$$\min\{\text{rank}(\boldsymbol{\Lambda}_{(a,b)})\} \le K \min\{N_{\mathrm{t}}N_{\mathrm{r}}T(L+1), N_{\mathrm{r}}TN_{\mathrm{C}}\} \le \text{rank}(\boldsymbol{R}_{\overline{\boldsymbol{H}}}) \quad (7)$$

For the system under investigation, the rank r is actually a function of the Hamming or free distance d of ECC, the mapping τ of the ECC-coded bit stream into different STFBs across the whole block, and the mapping σ of the ECC-coded bit stream into constellation symbols. The system diversity order is further bounded by

$$\min\{\text{rank}(\boldsymbol{\Lambda}_{(a,b)})\} \le \min\{K, d_{\min}\} \times \min\{N_{\mathrm{t}}N_{\mathrm{r}}T(L+1), N_{\mathrm{r}}TN_{\mathrm{C}}\} \le \text{rank}(\boldsymbol{R}_{\overline{\boldsymbol{H}}}) \quad (8)$$

where $d_{\min}$ is the minimum distance of the employed channel code. For block ECC, it refers to Hamming distance; for convolutional codes, it refers to free distance. Let us denote $r = f_{(d,\tau,\sigma)}$. If r and $\Pi_{c=1}^{r}\gamma_c$ are approximately the same for the same (d, τ, σ), the union bound for the average symbol error rate can be simplified as

$$\boldsymbol{P}_{\mathrm{e}} \le \sum_a \boldsymbol{P}_r(a)\sum_{b\ne a}\boldsymbol{P}_r\{\boldsymbol{M}_{(a)} - \boldsymbol{M}_{(b)}\} \simeq \sum_{(\tau,d,\sigma)}\frac{W_{(d,\tau,\sigma)}}{N_B}\binom{2f_{(d,\tau,\sigma)}-1}{f_{(d,\tau,\sigma)}}\left(\prod_{a=1}^{f_{(d,\tau,\sigma)}}\gamma_c^{(d,\tau,\sigma)}\right)^{-1}\left(\frac{\rho}{N_t}\right)^{-f_{(d,\tau,\sigma)}} \quad (9)$$

where $W_{(d,\tau,\sigma)}$ is the number of pairs of $\boldsymbol{M}_{(a)}$ and $\boldsymbol{M}_{(b)}$ with the same (d, τ, σ).

In order to demonstrate the relation between the diversity performance and the mapping τ more precisely, let us assume that the channels are independent over different CDC-based STFCs, then

$$\boldsymbol{\Lambda}_{(a,b)} = \psi_{(a,b)}(\boldsymbol{R}_{\overline{\boldsymbol{H}}^{(1)}}, \ldots, \boldsymbol{R}_{\overline{\boldsymbol{H}}^{(K)}})[\psi_{(a,b)}]^{\mathcal{H}} = (\boldsymbol{\Lambda}_{(a,b)}^{(1)}, \ldots, \boldsymbol{\Lambda}_{(a,b)}^{(K)})$$

where $\boldsymbol{\Lambda}_{(a,b)}^{(k)} = \psi_{(a,b)}^{(k)}\boldsymbol{R}_{\overline{\boldsymbol{H}}^{(k)}}[\psi_{(a,b)}^{(k)}]^{\mathcal{H}}$. In what follows, we discuss the mapping τ of the ECC-coded bit stream into different STFBs across the whole block.

1. *Case 1.* Assume $N_{\mathrm{F}} \ge N_{\mathrm{T}}(L+1)$, and full diversity space-time-frequency CDC, which achieves the upper bound of $\text{rank}(\Lambda_{(a,b)}^{(i,k)})$ for any pairs of channel-coded streams, is chosen, for each STFB.

Note that

$$\text{rank}(\boldsymbol{\Lambda}_{(a,b)}^{(i,k)}) \le \min\{N_{\mathrm{t}}N_{\mathrm{r}}T(L+1), N_rTN_{\mathrm{C}}\} \le \text{rank}(\boldsymbol{R}_{\overline{\boldsymbol{H}}^{(i,k)}})$$

In this case

$$\min\{\text{rank}(\boldsymbol{\Lambda}_{(a,b)}^{(k)})\} = \min\{\text{rank}(\boldsymbol{\Lambda}_{(a,b)}^{(i,k)})\}$$

Apparently, increasing the number of STFBs per CDC-based STFC to $N_a > 1$ will not increase the diversity order, which is $\min_{(a,b)}\{\text{rank}(\boldsymbol{\Lambda}_{(a,b)}^{(k)})\}$ for the kth CDC-based STFC. However, there might be some coding gain through channel coding. In this case, $N_a = 1$ is the best choice for exploiting diversity, that is, one-channel code stream is across multiple STFCs, and the part of the stream with one CDC-based STFC is only encoded in one STFB. However, since this may introduce long delay for long-channel codes, $N_a > 1$ may still be a practical choice.

2. *Case 2.* Assume $N_{\mathrm{F}} < N_{\mathrm{T}}(L+1)$, and a non-full-diversity space-time-frequency CDC is chosen for each STFB. In this case, $N_a > 1$ will increase the diversity order of the kth CDC-based STFC.

One further issue is to choose the number of units (such as symbols or bits) of one-channel code stream to be allocated to each STFB. Now we have the following proposition.

Proposition 1: One STF communications channel is of full rank over space, time and frequency, and is independent over different STFBs in time. Consider a joint 3D CDC and channel coding system. The physical dimensions of 3D CDC STFBs are sufficient to achieve full diversity over space, time and frequency. The channel-coding sequences operate in units (either bits or symbols). There are N_u channel-coding sequences, and each of them is of length K units and with minimum pairwise distance $d_{\min} \le K$ units to be encoded into K STFBs. If one STFB only encodes a single unit of each channel-coding sequence, the system achieves the diversity order upper bound

$$\min\{\text{rank}(\boldsymbol{\Lambda}_{(a,b)})\} = d_{\min}\min\{N_{\mathrm{t}}N_{\mathrm{r}}T(L+1), N_{\mathrm{r}}TN_{\mathrm{C}}\}$$

doi: 10.1049/iet-spr.2010.0196

Proof: Note that

$$\begin{aligned}\boldsymbol{\Lambda}_{(a,b)} &= \phi_{(a,b)}\text{diag}(\boldsymbol{R}_{\overline{\boldsymbol{H}}^{(1)}}, \ldots, \boldsymbol{R}_{\overline{\boldsymbol{H}}^{(K)}})[\phi_{(a,b)}]^{\mathcal{H}} \\ &= \text{diag}(\boldsymbol{\Lambda}_{(a,b)}^{(1)}, \ldots, \boldsymbol{\Lambda}_{(a,b)}^{(K)}), \\ &= \text{diag}(\psi_{(a,b)}^{(1)}\boldsymbol{R}_{\overline{\boldsymbol{H}}^{(1)}}[\psi_{(a,b)}^{(1)}]^{\mathcal{H}}, \ldots, \psi_{(a,b)}^{(K)}\boldsymbol{R}_{\overline{\boldsymbol{H}}^{(K)}}[\psi_{(a,b)}^{(K)}]^{\mathcal{H}})\end{aligned}$$

Thus

$$\text{rank}(\boldsymbol{\Lambda}_{(a,b)}) = \sum_{k=1}^{K} \psi_{(a,b)}^{(k)}\boldsymbol{R}_{\overline{\boldsymbol{H}}^{(k)}}[\psi_{(a,b)}^{(k)}]^{\mathcal{H}}$$

Because each channel-coding sequence has minimum pairwise distance $d_{\min} \leq K$ units, there are differences of $d_{\min}$ units for any two different information sequences. Note that one STFB only encodes a single unit of each channel-coding sequence, so that there are at least $d_{\min}$ STFBs with different channel-coded input for any two different information sequences. Hence

$$\begin{aligned}\min\{\text{rank}(\boldsymbol{\Lambda}_{(a,b)})\} &= d_{\min}\text{rank}\{\psi_{(a,b)}^{(1)}\boldsymbol{R}_{\overline{\boldsymbol{H}}^{(1)}}[\psi_{(a,b)}^{(1)}]^{\mathcal{H}}\} \\ &= d_{\min}\min\{N_{\text{t}}N_{\text{r}}T(L+1), N_{\text{r}}TN_{\text{C}}\}\end{aligned} \quad (10)$$

□

The coded diversity system described in Proposition 1 actually encodes N_u channel-coded streams of K units in parallel. If the unit is one bit, we call it bit-interleaved coded complex diversity coding (BICCDC)-based approach. Bit-interleaved coded modulation (BICM) is different from BICCDC, since in BICM, bits are interleaved simply across different constellation symbols. If the unit is one symbol, we call the corresponding approach symbol-interleaved coded complex diversity coding (SICCDC).

4 Iterative decoding of CDC–ECC STFC

Fig. 4 depicts the iterative CDC–ECC STFC decoding scheme. The STFC decoder takes channel observation vector $\boldsymbol{y}$ and a priori information $\lambda(c'; I)$ on the coded and interleaved bits c' and computes its extrinsic information $\lambda(c'; O)$, which is subsequently de-interleaved to $\lambda(c; I)$. With a priori input $\lambda(c; I)$, a soft-input, soft-output (SISO) ECC decoder computes log-likelihood ratio (LLR) $\lambda(c; O)$ for the coded bits and $\lambda(b; O)$ for the information bits. The latter is used at the final iteration to make a hard decision on the transmitted information bits; whereas the former is interleaved and fed back to the STFC decoder as a priori information. Several SISO algorithms can be applied to compute the ECC decoder output. For the purpose of this study, we consider the use of the Log-MAP algorithm [10].

Recall that the received signal vector is expressed as $\boldsymbol{y} = \sqrt{\rho/N_{\text{t}}}\boldsymbol{HGs} + \boldsymbol{n}$. The transmitted symbol vector $\boldsymbol{s}$ can

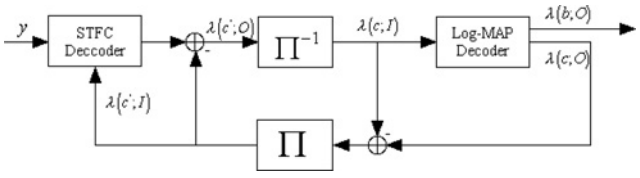

Fig. 4 *Structure of the iterative STFC decoding*

be estimated by a linear MMSE algorithm, that is

$$\boldsymbol{z} = \boldsymbol{W}^H\boldsymbol{y} = \boldsymbol{W}^H\left(\sqrt{\frac{\rho}{N_{\text{t}}}}\boldsymbol{HGs} + \boldsymbol{n}\right) = \boldsymbol{Us} + \boldsymbol{v} \quad (11)$$

where the matrix $\boldsymbol{W}$ is designed to minimise the mean-square error $e = \text{E}[\|\boldsymbol{z} - \boldsymbol{s}\|^2]$, leading to the solution $\boldsymbol{W} = \boldsymbol{R}^{-1}\boldsymbol{P}$, where

$$\begin{aligned}\boldsymbol{R} = \text{E}[\boldsymbol{yy}^H] &= \boldsymbol{E}\left[\frac{\rho}{N_{\text{t}}}(\boldsymbol{HGs} + \boldsymbol{n})(\boldsymbol{s}^H\boldsymbol{G}^H\boldsymbol{H}^H + \boldsymbol{n}^H)\right] \\ &= \frac{\rho}{N_{\text{t}}}\boldsymbol{HH}^H + N_0\boldsymbol{I}\end{aligned} \quad (12)$$

$$\begin{aligned}\boldsymbol{P} = \text{E}[\boldsymbol{ys}^H] &= \text{E}\left[\sqrt{\frac{\rho}{N_{\text{t}}}}\boldsymbol{HGs} + \boldsymbol{n})\boldsymbol{s}^H\right] = \sqrt{\frac{\rho}{N_{\text{t}}}}\boldsymbol{HG}; \\ \boldsymbol{U} &= \boldsymbol{W}^H\boldsymbol{P}\end{aligned} \quad (13)$$

Equation (12) is derived utilising the fact that $\boldsymbol{G}$ is a unitary matrix.

The noise term $\boldsymbol{v}$ is Gaussian since it is a linear transformation of a Gaussian random vector $\boldsymbol{n}$ ($\boldsymbol{v} = \boldsymbol{W}^H\boldsymbol{n}$), with zero mean and covariance $\Gamma = \text{E}[\boldsymbol{vv}^H] = N_0\boldsymbol{W}^H\boldsymbol{W}$. Because the filtered noise $\boldsymbol{v}$ is no longer white (Γ is not an identity matrix, the elements of $\boldsymbol{v}$ are correlated), optimum detection involves joint estimation of all the symbols in the vector $\boldsymbol{s}$, which requires ML or near-ML sphere decoding. However, we have observed from our experiments that the off-diagonal elements of Γ are quite small compared with the diagonal elements. Therefore we can well approximate Γ as a diagonal matrix. Consequently, each element of $\boldsymbol{s}$ can be estimated individually, and the receiver design is greatly simplified. The kth element of $\boldsymbol{z}$, denoted by z_k, can be written as $z_k = u_k s_k + v_k$, where u_k is the kth diagonal element of $\boldsymbol{U}$, and s_k, v_k are the kth elements of the vectors $\boldsymbol{s}$, $\boldsymbol{v}$, respectively. The noise term v_k is a Gaussian random variable with zero mean and variance N_k, which is the kth diagonal element of the matrix Γ. The probability density function (PDF) of the MMSE filter output z_k, conditioned on that the mth PSK/QAM symbol is transmitted, can be expressed as

$$f(z_k|s_m) = \frac{1}{\pi N_k}\exp\left(-\frac{|z_k - u_k s_m|^2}{N_k}\right) \quad (14)$$

In what follows, we derive a general expression for symbol-to-bit LLR mapping scheme based on the PDF function expressed by (14) for different modulation schemes. For a PSK/QAM system, we need to compute LLRs for M coded bits for each symbol s_k, which is one of the $r = 2^M$ possible symbols in the signal constellation. For example, $M = 2$ for QPSK, and $M = 4$ for 16-QAM. Denote the transmitted symbol $s_k = \text{map}\{c_k^{0'}, c_k^{1'}, \ldots, c_k^{(M-1)'}\}|_{c_k^{m'} \in \{0,1\}}$, the LLR value of the bit $c_k^{m'}$ conditioned on the MMSE filter output z_k can be calculated as

$$\lambda(c_k^{m'}|z_k) = \ln\frac{\Pr(c_k^{m'} = 1|z_k)}{\Pr(c_k^{m'} = 0|z_k)} \quad (15)$$

To simplify (15), we define $\boldsymbol{I}_{+m}$ and $\boldsymbol{I}_{-m}$ for $m = 0$ as

$$I_{-0} = \underbrace{\begin{pmatrix} 0 & 0 & \cdots & 0 & 0 \\ 0 & 0 & \cdots & 0 & 1 \\ \vdots & \vdots & \ldots & \vdots & \vdots \\ 0 & 0 & \cdots & 1 & 1 \\ 0 & 1 & \cdots & 0 & 1 \end{pmatrix}}_{M \times 2^{M-1}};$$

$$I_{+0} = \underbrace{\begin{pmatrix} 1 & 1 & \cdots & 1 & 1 \\ 0 & 0 & \cdots & 0 & 1 \\ \vdots & \vdots & \ldots & \vdots & \vdots \\ 0 & 0 & \cdots & 1 & 1 \\ 0 & 1 & \cdots & 0 & 1 \end{pmatrix}}_{M \times 2^{M-1}} \tag{16}$$

Note that for $m = 0$, the first row of matrix $\boldsymbol{I}_{-0}$ has all elements equal to 0, while the first row of matrix $\boldsymbol{I}_{+0}$ has all elements equal to 1. The other matrices for $m = 1, 2, \ldots, M-1$ can be found by exchanging the first row with the corresponding $(m+1)$th row. Using Bayes' theorem, we can write (15) as

$$\lambda(c_k^{m'}|z_k) = \lambda(c_k^{m'}) + \ln \frac{\sum_{p=0}^{2^{M-1}} p(z_k|\text{map}\{\boldsymbol{i}_{+mp}\}) e^{\boldsymbol{L}\boldsymbol{i}_{\text{mp}}}}{\sum_{p=0}^{2^{M-1}} p(z_k|\text{map}\{\boldsymbol{i}_{-\text{mp}}\}) e^{\boldsymbol{L}\boldsymbol{i}_{\text{mp}}}} \tag{17}$$

where $\boldsymbol{i}_{+\text{mp}}$ and $\boldsymbol{i}_{-mp}$ are $(p+1)$th column vectors of matrices $\boldsymbol{I}_{+m}$ and $\boldsymbol{I}_{-m}$. In (17), $\boldsymbol{i}_{\text{mp}}$ is the $(p+1)$th column vector of matrix $\boldsymbol{I}_{+m}$ with its mth entry set equal to zero, and $\boldsymbol{L} = [\lambda(c_k^{0'})\lambda(c_k^{1'}) \ldots \lambda(c_k^{(M-1)'})]$ is a row vector of a posteriori LLRs, The second term in (17) is the extrinsic information of bit $c_{k,}^{m}$. Denoting the extrinsic information of the mth bit by $\lambda_{\text{e}}(c_k^{m})$, we have

$$\lambda_{\text{e}}(c_k^{m'}) = \ln \frac{\sum_{p=0}^{2^{M-1}} p(z_k|\text{map}\{i_{+\text{mp}}\}) e^{\mathbf{L}\mathbf{i}_{\text{mp}}}}{\sum_{p=0}^{2^{M-1}} p(z_k|\text{map}\{i_{-\text{mp}}\}) e^{\mathbf{L}\mathbf{i}_{\text{mp}}}} \tag{18}$$

Substituting (14) into (18) yields

$$\begin{aligned} \lambda_{\text{e}}(c_k^{m'}) = & \max^* \left\{ \frac{-|z_k - u_k \text{map}\{i_{+m0}\} \boldsymbol{L}\boldsymbol{i}_{m0}|^2}{N_k}, \ldots, \right. \\ & \left. \frac{-|z_k - u_k \text{map}\{i_{+m(P-1)}\} \boldsymbol{L}\boldsymbol{i}_{m(P-1)}|^2}{N_k} \right\} \\ & - \max^* \left\{ \frac{-|z_k - u_k \text{map}\{i_{-m0}\} \boldsymbol{L}\boldsymbol{i}_{m0}|^2}{N_k}, \ldots, \right. \\ & \left. \frac{-|z_k - u_k \text{map}\{i_{-m(P-1)}\} \boldsymbol{L}\boldsymbol{i}_{m(P-1)}|^2}{N_k} \right\} \end{aligned} \tag{19}$$

where $\max^*[]$ is defined as $\max^*[x, y] = \ln(e^x + e^y) = \max[x, y] + \ln(1 + e^{-|x-y|})$, that is, the max operation compensated with a correction term $\ln(1 + e^{-|x-y|})$. Also $\max^*[x, y, z] = \max^*[\max^*[x, y], z]$, etc.

In the case of QPSK modulation, each QPSK symbol s_k corresponds to two coded bits $c_k^{0'}$ and $c_k^{1'}$. Equation (18) is simplified to [11]

$$\lambda_{\text{e}}(c_k^{0'}) = \frac{\ln P_r(z_k|c_k^{0'}=1, c_k^{1'}=0) + P_r(z_k|c_k^{0'}=1, c_k^{1'}=1) e^{L_a(c_k^{1'})}}{P_r(z_k|c_k^{0'}=0, c_k^{1'}=0) + P_r(z_k|c_k^{0'}=0, c_k^{1'}=1) e^{L_a(c_k^{1'})}} \tag{20}$$

where $L_a(c_k^{1'})$ is the a priori value for the bit $c_k^{1'}$. Substituting (14) into (20) yields

$$\begin{aligned} \lambda_{\text{e}}(c_k^{0'}) = & \max^* \left\{ -\frac{|z_k - u_k s_{10}|^2}{N_k}, -\frac{|z_k - u_k s_{11}|^2}{N_k} + L_a(c_k^{1'}) \right\} \\ & - \max^* \left\{ -\frac{|z_k - u_k s_{00}|^2}{N_k}, -\frac{|z_k - u_k s_{01}|^2}{N_k} + L_a(c_k^{1'}) \right\} \end{aligned}$$

where s_{mn} denotes the symbol corresponding to the bits $c_k^{0'} = m$, and $c_k^{1'} = n$. Similarly

$$\begin{aligned} \lambda_{\text{e}}(c_k^{1'}) \simeq & \max^* \left\{ -\frac{|z_k - u_k s_{01}|^2}{N_k}, -\frac{|z_k - u_k s_{11}|^2}{N_k} + L_a(c_k^{0'}) \right\} \\ & - \max^* \left\{ -\frac{|z_k - u_k s_{00}|^2}{N_k}, -\frac{|z_k - u_k s_{10}|^2}{N_k} + L_a(c_k^{1'}) \right\} \end{aligned}$$

Two bit-to-symbol mapping schemes, namely, Gray and anti-Gray are considered in this work, for QPSK and 16-QAM systems, respectively. The results will be shown in Section 5.

For a multi-stream system, the received signal can be written as

$$\boldsymbol{r} = \sum_{i=1}^{N_{\text{t}}} \sqrt{\frac{\rho}{N_{\text{t}}}} \boldsymbol{H}\boldsymbol{G}_i \boldsymbol{s}_i + \boldsymbol{n} \tag{21}$$

where $\boldsymbol{G}_i$ is the encoding matrix for the ith stream and $\boldsymbol{s}_i$ is the ith source symbol vector. In order to facilitate MMSE decoding, we reformulate (21) as

$$\begin{aligned} \boldsymbol{r} = \sum_{i=1}^{N_{\text{t}}} \sqrt{\frac{\rho}{N_{\text{t}}}} \boldsymbol{H}\boldsymbol{G}_i \boldsymbol{s}_i + \boldsymbol{n} &= \sqrt{\frac{\rho}{N_{\text{t}}}} \sum_{i=1}^{N_{\text{t}}} \boldsymbol{H}_i \boldsymbol{s}_i + \boldsymbol{n} \\ &= \sqrt{\frac{\rho}{N_{\text{t}}}} \underbrace{[\boldsymbol{H}_1 \quad \cdots \quad \boldsymbol{H}_{N_{\text{t}}}]}_{\boldsymbol{H}_{\text{eq}}} \underbrace{\begin{bmatrix} \boldsymbol{s}_1 \\ \vdots \\ \boldsymbol{s}_{N_{\text{t}}} \end{bmatrix}}_{\boldsymbol{s}_{\text{eq}}} + \boldsymbol{n} \end{aligned} \tag{22}$$

where $\boldsymbol{H}_i = \boldsymbol{H}\boldsymbol{G}_i$. The rest of the derivation follows similarly to (11)–(18), with $\boldsymbol{H}\boldsymbol{G}$ replaced by $\boldsymbol{H}_{\text{eq}}$, and $\boldsymbol{s}$ replaced by $\boldsymbol{s}_{\text{eq}}$.

5 Numerical results

Simulation settings are summarised as follows:

1. A convolutional code (with block size of 512 coded bits, code rate $R_{\text{c}} = 1/2$, constraint length 3, and generator polynomials (5, 7) in octal form) is used in Figs. 5–7; a Reed Solomon code (each RS codeword includes 6 RS information symbols and two redundancy symbols, and each RS symbol corresponds to 4 bits) is used in Fig. 8.

doi: 10.1049/iet-spr.2010.0196

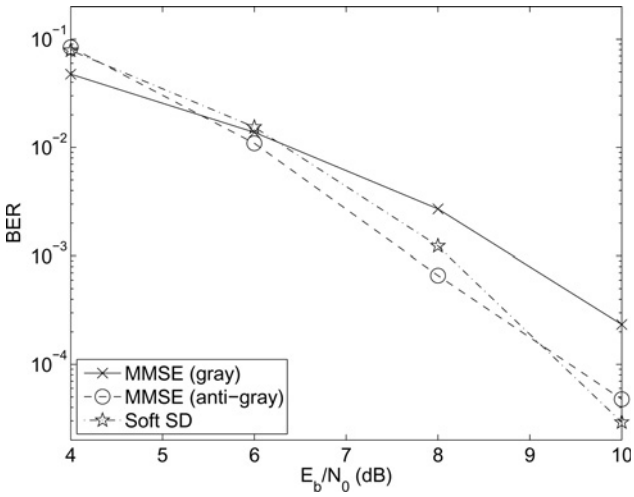

Fig. 5 *Performance comparison of MMSE and SD in ECC–STFC system with QPSK modulation*

MMSE with Gray mapping and soft SD decoding schemes are non-iterative. The curve for MMSE with anti-Gray mapping is plotted at the fourth iteration

2. MIMO frequency selective channel has channel order $L = 1$ (two-path except in Fig. 6*b* where seven-path channel is assumed), and each path experiences independent Rayleigh fading. Channel power delay profile is assumed to be uniform.
3. $N_t = N_r = 2$, $N_F = 4$, $T = 2$ and $N_C = 32$.
4. The number of STFCs for joint CDC and ECC is K, and the number of STFBs within one STFC for one block of 3D CDC and ECC is N_a.

Performance of different decoding algorithms for the joint CDC–ECC system with QPSK modulation are demonstrated in Fig. 5. Comparing the two non-iterative schemes, soft SD [6] shows 1 dB gain at BER $= 10^{-4}$ compared to the MMSE scheme with Gray mapping. However, we observed that the performance of the MMSE decoding can be much improved by using anti-Gray mapping and iterative decoding, which is slightly better than or comparable to the non-iterative soft SD decoding over a wide range of signal-to-noise ratios (SNRs).

Fig. 6 shows the performance of the MMSE decoding for 16-QAM modulated CDC–ECC STFC system with Gray and anti-Gray mapping for two-path and seven-path channels, respectively. For the anti-Gray system, there is a significant performance improvement by applying an iterative process if we compare the topmost curve representing the first iteration of CDC-based STFC MMSE decoding and Log-MAP ECC decoding with the bottom curve representing the performance of iterative decoding upon convergence. The most significant gain is obtained at the second iteration. Note that no gain can be obtained by performing the iterative process for the systems with Gray mapping, in which the bits are mapped to I and Q channels independently [11]. The iterative MMSE decoding with anti-Gray mapping outperforms the one with Gray mapping at the fourth iteration when $E_b/N_0 > 26.1$ dB and $E_b/N_0 > 22.2$ dB for two-path and seven-path channels, respectively. This suggests that if the 16-QAM system operates at low SNR, Gray mapping can be applied. Otherwise, anti-Gray mapping and iterative decoding would be preferred. By comparing Fig. 6*a* with *b*, it is evident that the proposed system can exploit the diversity gain provided by multipth propagation.

Fig. 7 shows the performance comparison between ECC-only STFCs and iterative CDC–ECC STFCs as well as the impact of the parameter N_a on the STFC system performance. To maintain the same data rates among ECC-only STFCs and iterative CDC–ECC STFCs, we construct ECC-only STFCs by using identity matrices for $\boldsymbol{G}_{\text{STFB}}$ in CDC-based STFCs. Clearly, iterative CDC–ECC STFCs outperform ECC-only STFCs, especially at higher SNRs and when the iterative scheme converges. Consistent with the analysis in Section 3 (in Fig. 7), the system using full diversity 3D CDC-based STFC with $N_a = 1$ outperforms that with $N_a = 4$.

Fig. 8 shows the results of joint full diversity 3D CDC and ECC with Reed–Solomon (RS) codes. Each RS-coded stream is across N_a 3D CDC STFCs, and one RS codeword is only across one STFB within each STFC. The number of RS symbols of one RS codeword within one STFB is N_g. In the simulations, hard SD for 3D CDC STFCs and hard decisions for RS codes are chosen. From Fig. 8, one can see that with the same configurations of RS codewords,

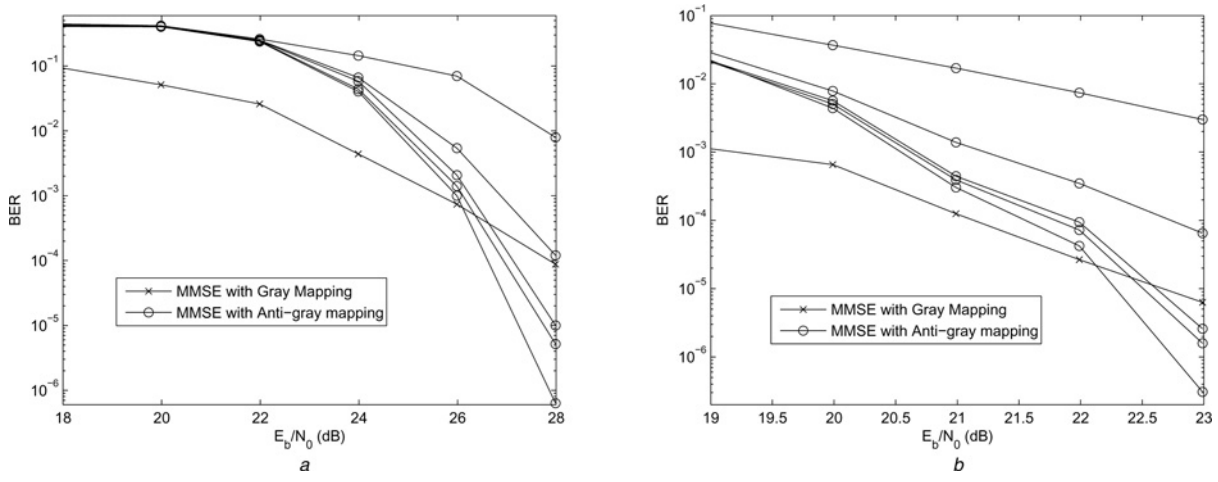

Fig. 6 *Performance of iterative MMSE decoding*

Employed modulation scheme is 16-QAM. For the systems with anti-Gray mapping, the top curve represents the first iteration of the CDC–ECC decoding, and the bottom curve represents the fifth iteration of the CDC–ECC decoding.
a Two-path channel
b Seven-path channel

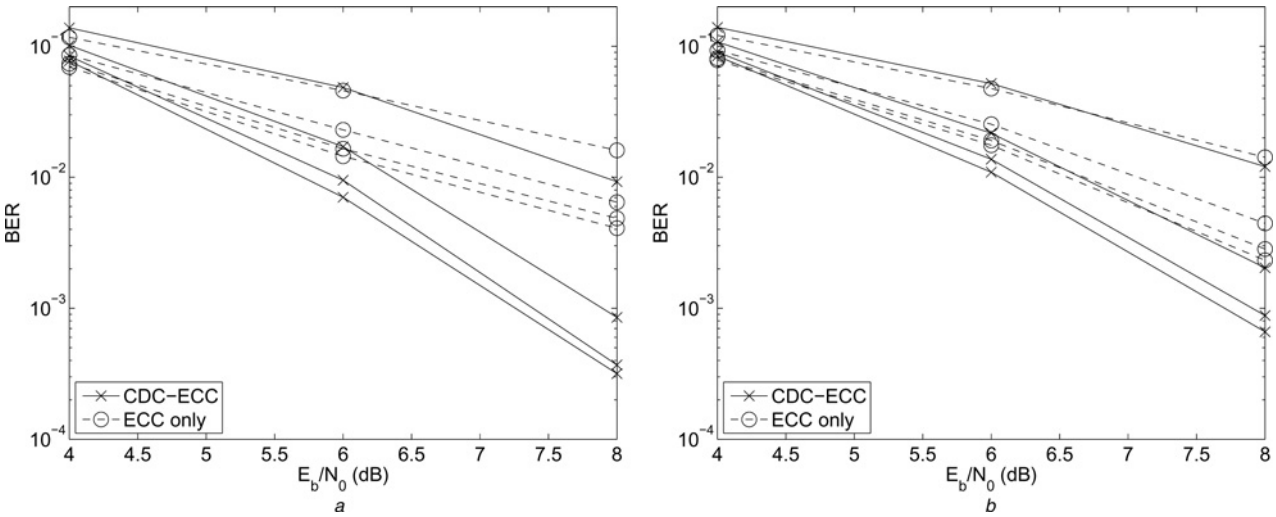

Fig. 7 *STFC performance comparisons between iterative CDC–ECC and ECC-only*

The top curve represents the first iteration, the bottom curve represents the fourth iteration
a $N_a = 1$
b $N_a = 4$

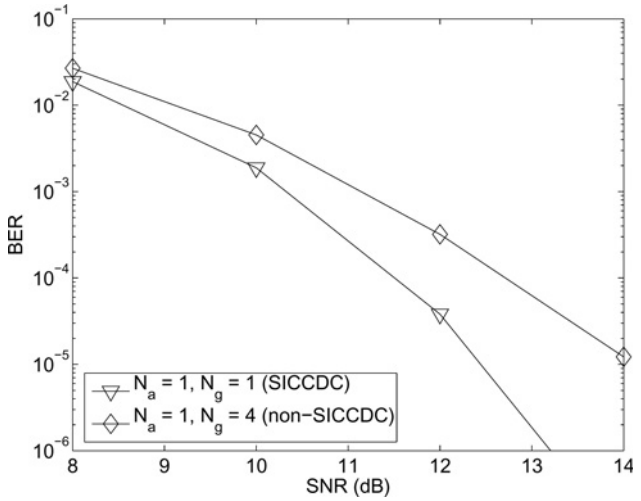

Fig. 8 *Effect of using SICCDC on the performance of joint 3D CDC and RS codes*

STFC using SICCDC, that is, $N_g = 1$ significantly outperforms STFC without SICCDC, that is, $N_g = 4$. Considering the case when a pair of RS codewords have the minimum distance, that is, two RS symbols, the probability of two different RS symbols being encoded into two different STFBs over time is (i) one in the SICCDC case; (ii) 4/7 in the case without using SICCDC. As shown by (10), for the SICCDC case, $\min\{\text{rank}(\Lambda_{(a,b)})\} = 2\min\{N_t N_r T(L+1) N_r T N_C\}$; whereas for the case without SICCDC, $\min\{\text{rank}(\Lambda_{(a,b)})\} = \min\{N_t N_r T(L+1), N_r T N_C\}$. Note that they are the lower bounds, and when a pair of RS codewords differ in more than two RS symbols, $\text{rank}(\Lambda_{(a,b)})$ may be much higher than $\min\{\text{rank}(\Lambda_{(a,b)})\}$ in the SICCDC case. It is observed from Fig. 8 that the SICCDC with full diversity, proved in Section 3, yields superior performance because of its better diversity properties.

6 Conclusions

Joint 3D space-time-frequency CDC and channel coding has been investigated in this paper. Our theoretical analysis reveals that by exploiting diversities over all three physical dimensions (spatial, time and frequency), the joint code design has the potential to achieve a diversity order of $\min\{K, d_{\min}\}\min\{N_t N_r T(L+1), N_r T N_C\}$, where N_t is the number of transmit antenna, N_r is the number of receive antennas, N_c is the number of subcarriers per antennas, L is the frequency selective channel order between any pair of transmit and receive antennas, $d_{\min}$ is the minimum distance of the employed channel code, and K is the number of 3D CDC over time. This paper proposes and proves full diversity construction with 3D CDC and channel coding, BICCDC and SICCDC.

The iterative decoding of ECC and CDC has been investigated in order to exploit the diversity potential inherent in the joint CDC–ECC STFC system. In particular, a low-complexity MMSE iterative decoding scheme with anti-Gray mapping is proposed, and is shown to achieve the performance of soft sphere decoding, and at the same time, reduce the complexity from exponential to polynomial. A multi-stream CDC–ECC architecture is also introduced and is shown to have comparable performance to a single-stream system with reduced complexity and decoding latency because of its parallel structure.

7 References

1 Liu, Z., Giannakis, G.: 'Space-time-frequency coded OFDM over frequency-selective fading channels', *IEEE Trans. Signal Process.*, 2002, **50**, (10), pp. 2465–2476
2 Zhang, W., Xia, X., Ching, P.: 'High-rate full-diversity space-time-frequency codes for broadband MIMO block-fading channels', *IEEE Trans. Commun.*, 2007, **55**, (1), pp. 25–34
3 Boutros, J., Viterbo, E.: 'Signal space diversity: a power- and bandwidth-efficient diversity technique for the Rayleigh fading channel', *IEEE Trans. Inf. Theory*, 1998, **44**, (4), pp. 1453–1467
4 Su, W., Safar, Z., Liu, K.: 'Towards maximum achievable diversity in space, time, and frequency: performance analysis and code design', *IEEE Trans. Wirel. Commun.*, 2005, **4**, (4), pp. 1847–1857
5 Wang, Z., Zhou, S., Giannakis, G.: 'Joint coding-precoding with low-complexity turbo-decoding', *IEEE Trans. Wirel. Commun.*, 2004, **3**, (3), pp. 832–842
6 Wang, R., Ma, X., Giannakis, G.: 'Improving the performance of coded FDFR multi-antenna systems with turbo-decoding', *Wirel. Commun. Mob. Comput.*, 2004, **4**, pp. 711–725
7 Wang, R., Giannakis, G.: 'Approaching MIMO channel capacity with reduced-complexity soft sphere decoding', *Proc. IEEE WCNC*, 2004, **3**, pp. 1620–1625

doi: 10.1049/iet-spr.2010.0196

8 Hassibi, B., Hochwald, B.: 'High-rate codes that are linear in space and time', *IEEE Trans. Inf. Theory*, 2002, **48**, (7), pp. 1804–1824
9 Siwamogsatham, S., Fitz, M., Grimm, J.: 'New view of performance analysis of transmit diversity schemes in correlated Rayleigh fading', *IEEE Trans. Inf. Theory*, 2002, **48**, (4), pp. 950–956
10 Robertson, P., Hoeher, P., Villebrum, E.: 'Optimal and sub-optimal maximum a posteriori algorithms suitable for Turbo decoding', *Eur. Trans. Telecommun.*, 1997, **8**, (2), pp. 119–125
11 Brink, S., Speidel, J., Yan, R.: 'Iterative demapping for QPSK modulation', *Electron. Lett.*, 1998, **34**, (15), pp. 1459–1460